COLD REGULATED 27 and 28 are targets of CONSTITUTIVELY PHOTOMORPHOGENIC 1 and negatively affect phytochrome B signalling

Nikolai Kahle[1], David J. Sheerin[1], Patrick Fischbach[2], Leonie-Alexa Koch[2], Philipp Schwenk[1,3], Dorothee Lambert[1], Ryan Rodriguez[1], Konstantin Kerner[4], Ute Hoecker[4], Matias D. Zurbriggen[2] (iD) and Andreas Hiltbrunner[1,5,*] (iD)

[1]*Institute of Biology II, Faculty of Biology, University of Freiburg, Freiburg 79104, Germany,*

[2]*Institute of Synthetic Biology and CEPLAS, Heinrich Heine University Düsseldorf, Düsseldorf 40225, Germany,*

[3]*Spemann Graduate School of Biology and Medicine (SGBM), University of Freiburg, Freiburg 79104, Germany,*

[4]*Institute for Plant Sciences, University of Cologne, Cologne 50674, Germany, and*

[5]*Signalling Research Centres BIOSS and CIBSS, University of Freiburg, Freiburg 79104, Germany*

SUMMARY

Phytochromes are red/far-red light receptors in plants involved in the regulation of growth and development. Phytochromes can sense the light environment and contribute to measuring day length; thereby, they allow plants to respond and adapt to changes in the ambient environment. Two well-characterized signalling pathways act downstream of phytochromes and link light perception to the regulation of gene expression. The CONSTITUTIVELY PHOTOMORPHOGENIC 1/SUPPRESSOR OF PHYA-105 (COP1/SPA) E3 ubiquitin ligase complex and the PHYTOCHROME INTERACTING FACTORs (PIFs) are key components of these pathways and repress light responses in the dark. In light-grown seedlings, phytochromes inhibit COP1/SPA and PIF activity and thereby promote light signalling. In a yeast-two-hybrid screen for proteins binding to light-activated phytochromes, we identified COLD-REGULATED GENE 27 (COR27). COR27 and its homologue COR28 bind to phyA and phyB, the two primary phytochromes in seed plants. COR27 and COR28 have been described previously with regard to a function in the regulation of freezing tolerance, flowering and the circadian clock. Here, we show that COR27 and COR28 repress early seedling development in blue, far-red and in particular red light. COR27 and COR28 contain a conserved Val-Pro (VP)-peptide motif, which mediates binding to the COP1/SPA complex. COR27 and COR28 are targeted for degradation by COP1/SPA and mutant versions with a VP to AA amino acid substitution in the VP-peptide motif are stabilized. Overall, our data suggest that COR27 and COR28 accumulate in light but act as negative regulators of light signalling during early seedling development, thereby preventing an exaggerated response to light.

Keywords: phytochrome, photomorphogenesis, COP1, SPA1, protein degradation, signal integration.

INTRODUCTION

Light strongly affects the growth and development of plants, reaching from induction of germination and early seedling development to transition from the vegetative to the reproductive state, and senescence. As such, light is one of the most important environmental factors that regulate the life cycle of plants. Plants evolved an intriguing and complex signalling network to monitor precisely the light quality and quantity to adapt to their ambient surroundings (Kami *et al.*, 2010). *Arabidopsis thaliana* contains five families of photoreceptors that provide input to this signalling network. UV RESISTANCE 8 (UVR8), phototropins, cryptochromes, members of the ZEITLUPE protein family, and phytochromes sense light of different qualities and regulate distinct and overlapping light responses in Arabidopsis. The phytochrome family (phy) consists of five members, phyA to phyE, and plays an essential role throughout life in sensing and responding to wavelengths in the red (R) and far-red (FR) range of the light spectrum (Paik and Huq, 2019). Phytochromes are synthesized in the cytosol in their inactive Pr form, which has an absorption peak at 660 nm and preferentially absorbs R light. Light absorption of phytochromes in the Pr form results in a conformational change to their physiologically active Pfr form, which subsequently translocates into the nucleus where it directly interacts

with several downstream signalling components (Legris *et al.*, 2019).

The two primary phytochrome downstream signalling pathways in the nucleus involve the CONSTITUTIVELY PHOTOMORPHOGENIC 1 (COP1)/SUPPRESSOR OF PHYA-105 (SPA) E3 ubiquitin ligase complex and a set of bHLH transcription factors, the PHYTOCHROME INTERACTING FACTORs (PIFs) (Hoecker, 2017; Lee and Choi, 2017; Podolec and Ulm, 2018; Paik and Huq, 2019). The COP1/SPA complex is active in darkness and ubiquitinates positive factors of photomorphogenesis, such as the transcription factor ELONGATED HYPOCOTYL 5 (HY5), leading to their degradation via the 26S proteasome (Osterlund *et al.*, 2000; Seo *et al.*, 2003; Laubinger *et al.*, 2004; Hoecker, 2005; Jang *et al.*, 2005; Hoecker, 2017). Light-activated phytochromes directly bind to COP1 and SPAs and inhibit their E3 ubiquitin ligase function (Yang *et al.*, 2001; Seo *et al.*, 2004; Saijo *et al.*, 2008; Jang *et al.*, 2010; Lau and Deng, 2012; Viczián *et al.*, 2012; Lu *et al.*, 2015; Sheerin *et al.*, 2015; Podolec and Ulm, 2018). Additionally, COP1 is excluded from the nucleus upon prolonged light irradiation (von Arnim and Deng, 1994; Pacín *et al.*, 2013; Pacín *et al.*, 2014; Balcerowicz *et al.*, 2017). Light-dependent reduction of COP1/SPA activity results in the accumulation of their downstream targets and a subsequent change in gene expression (Lau and Deng, 2012). However, the function of COP1 is not limited to phytochrome signalling. Similar mechanisms of COP1 regulation are also described for UVR8 and cryptochromes (Podolec and Ulm, 2018; Ponnu *et al.*, 2019; Lau *et al.*, 2019), and COP1 is involved in temperature signalling and mediates light input to the circadian clock by regulating the stability of GIGANTEA (GI) (Yu *et al.*, 2008; Jang *et al.*, 2015; Park *et al.*, 2017). The fact that homozygous knockout mutations of *COP1* are lethal further underlines the importance of COP1 as a signalling hub for various pathways and responses (McNellis *et al.*, 1994). Parallel to and partially dependent on COP1/SPA, the PIFs also repress light signalling. Light-activated phytochromes bind PIFs and repress their activity by promoting their phosphorylation and targeting for degradation as well as by inhibiting their association with target promoters (Bauer *et al.*, 2004; Shen *et al.*, 2005; Al-Sady *et al.*, 2006; Shen *et al.*, 2008; Park *et al.*, 2012; Lee and Choi, 2017; Pham *et al.*, 2018; Paik and Huq, 2019).

In an approach to elucidate further the complex network of light signalling components and their potential interplay with other signalling pathways, we performed a yeast-two-hybrid (Y2H) screen for interactors of light-activated phyA. In this screen, we identified COLD-REGULATED GENE 27 (COR27) as a potential interactor of phyA. *COR27* and its homologue, *COLD-REGULATED GENE 28* (*COR28*), are both transcriptionally regulated by light and the circadian clock and their expression is strongly elevated upon

exposure to cold temperatures (Mikkelsen and Thomashow, 2009; Li *et al.*, 2016). COR27 and COR28 are stabilized by blue light (B) and bind to chromatin of circadian clock-related genes (Li *et al.*, 2016). The *cor27-1 cor28-2* double mutant is late flowering and several genes involved in circadian rhythms and the transition to flowering are misregulated in *cor27-1 cor28-2* (Li *et al.*, 2016; Wang *et al.*, 2017). Additionally, COR27 and COR28 are involved in freezing tolerance (Li *et al.*, 2016).

Here, we report that COR27 and COR28 directly bind to phytochromes and play a role in phytochrome-dependent early seedling development. Additionally, we show that the COP1/SPA complex directly targets COR27 and COR28 for degradation, suggesting an additional pathway for light, temperature and circadian clock integration in Arabidopsis.

RESULTS

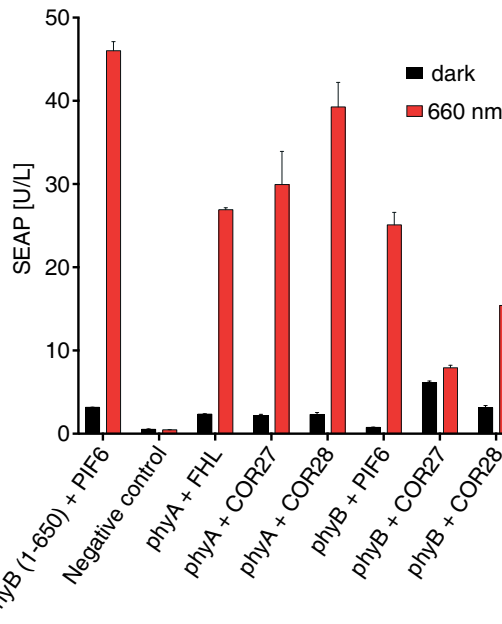### COR27 and COR28 interact with phyA and phyB

In a Y2H screen for phyA-interacting proteins, we identified COR27 as a potential interactor of phyA. We confirmed this finding in a subsequent Y2H growth assay and observed binding of the COR27 homolog, COR28, to phyA in yeast (Figure 1a). Additionally, we validated the interaction of COR27 and COR28 with phyA in a mammalian-two-hybrid (M2H) system in CHO-K1 cells (Figure 1b). To verify these interactions *in planta*, we generated stable transgenic *A. thaliana* lines expressing Pro35S:HA-YFP-COR27 (COR27ox) and Pro35S:HA-YFP-COR28 (COR28ox) and performed co-immunoprecipitation (CoIP) experiments, in which we could co-precipitate phyA with HA-YFP-COR27 and HA-YFP-COR28 using anti-green fluorescence protein (anti-GFP) antibody-coupled magnetic beads (Figure 1c). We also tested the interaction of COR27 and COR28 with phyB and observed binding of COR27 and COR28 to phyB in the Y2H as well as the M2H system (Figure 1a,b). Furthermore, we used lines co-expressing HA-YFP-COR27 and phyB-mCer for CoIP and could co-precipitate phyB-mCer with HA-YFP-COR27 (Figure 1d). All interaction assays were performed under conditions where phyA and phyB are either predominantly in their inactive Pr state (darkness or irradiation with FR light) or their active Pfr state (irradiation with R light). The Y2H approach suggests an enhanced interaction of COR27 with phyA and phyB Pfr compared with Pr, and in the M2H system, interactions between phyA and both COR27 and COR28, as well as between phyB and COR28 were enhanced when phytochromes were in the Pfr state. In addition, co-precipitation of phyA with HA-YFP-COR27 was enhanced after R light irradiation. Overall, our data suggest that COR27 and COR28 interact with phyA and phyB but in this study, we did not investigate further whether the interactions are Pfr/Pr-specific.
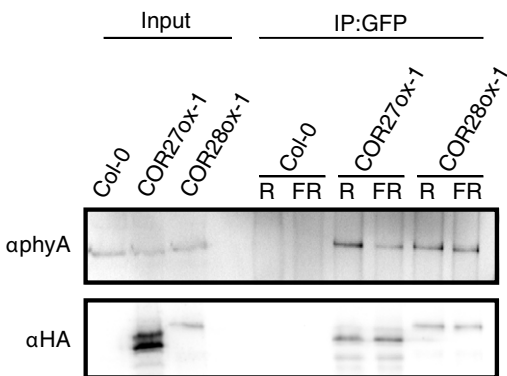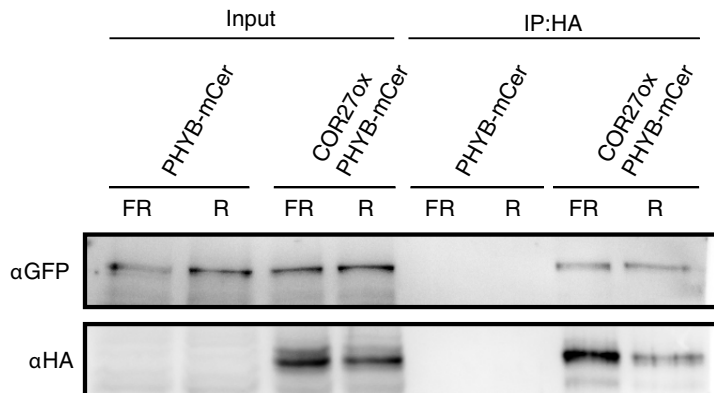
(a)
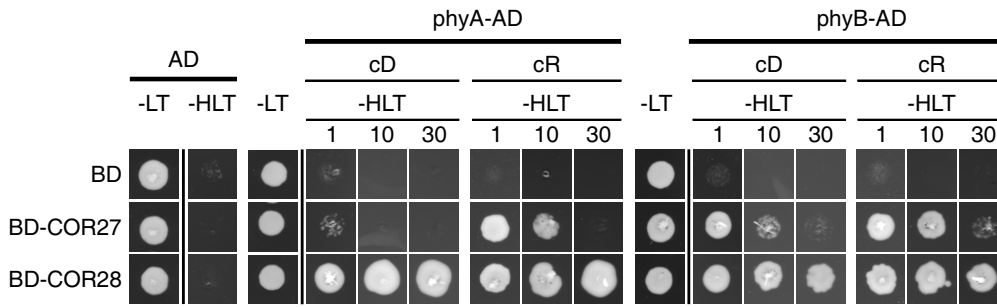
(b)

(c)

(d)

COR27 and COR28 are involved in light-dependent early seedling development

As COR27 and COR28 showed interaction with phyA and phyB, we investigated a potential role for COR27 and COR28 in phytochrome signalling. Therefore, we obtained the previously described T-DNA insertion lines *cor27-2*, a knockdown of *COR27*, and *cor28-2*, a knockout of *COR28* (Li *et al.*, 2016), and crossed these lines to obtain a *cor27-2 cor28-2* double mutant. We analysed the

Figure 1. COR27 and COR28 interact with phytochromes.

(a) Yeast-two-hybrid growth assay. Yeast cultures (strain AH109) co-expressing either COR27 or COR28 fused to the GAL4-DNA-binding domain (BD) and phyA or phyB fused to the GAL4-activation domain (AD) were grown on CSM -His -Leu -Trp (-HLT) plates containing 20 μM phycocyanobilin and 1, 10 or 30 mM 3-amino-1,2,4-triazole (1, 10, 30) to test for interaction. Plates were incubated for 7 days at 26°C either in darkness (cD) or in continuous red light (cR, 660 nm, 2 μmol m^{-2} sec^{-1}). Growth on CSM -Leu -Trp (-LT) plates was used as transformation control. FR, far-red light; R, red light.

(b) Mammalian-two-hybrid assay. CHO-K1 cells were transfected with a reporter plasmid coding for secreted alkaline phosphatase (SEAP) and vectors coding for phyA or phyB fused to the VP16 transactivation domain and COR27 or COR28 fused to the TetR DNA-binding domain. Cells were either kept in darkness or treated with R light (660 nm, 20 μmol m^{-2} sec^{-1}) for 24 h. The supernatant was used for SEAP activity measurements. Previously described interaction partners of phyA and phyB, FAR-RED-ELONGATED HYPOCOTYL1-LIKE (FHL) and PHYTOCHROME INTERACTING FACTOR 6 (PIF6), were used as positive controls.

(c) PhyA co-purifies with COR27 and COR28. Native protein extracts from 3-day-old, dark-grown Arabidopsis seedlings expressing Pro35S:HA-YFP-COR27 (COR27ox-1) or Pro35S:HA-YFP-COR28 (COR28ox-1) were treated with R light (680 nm, 5 μmol m^{-2} sec^{-1}) or FR light (780 nm, 5 μmol m^{-2} sec^{-1}) for 5 min and used for co-immunoprecipitation. Immunoprecipitation (IP) was performed using α-GFP-coupled magnetic beads. α-phyA and α-HA antibodies were used to detect endogenous phyA and HA-YFP-COR27 and HA-YFP-COR28.

(d) PhyB co-purifies with COR27. Four-day-old, dark-grown Arabidopsis seedlings expressing ProPHYB:phyB-mCer in *phyB-9* (PHYB-mCer) or Pro35S:HA-YFP-COR27 ProPHYB:phyB-mCer in *phyB-9* (COR27ox PHYB-mCer) were either treated with R light for 2 h (660 nm, 20 μmol m^{-2} sec^{-1}) or treated with R followed by a 5 min FR light pulse (760 nm, 20 μmol m^{-2} sec^{-1}) before harvesting. IP was performed using α-HA-coupled magnetic beads. α-GFP and α-HA antibodies were used to detect phyB-mCer and HA-YFP-COR27.

light response profile of the *cor27-2 cor28-2* double mutant by measuring hypocotyl length under different light qualities and photon fluence rates. The *cor27-2 cor28-2* double mutant was slightly hypersensitive to FR and B light, and showed strongly reduced hypocotyl growth compared with Columbia-0 (Col-0) wildtype when grown in R light (Figure 2; Figure S1). These findings suggest a function of COR27 and COR28 in B, FR and particularly R light induced photomorphogenesis. As the *cor27-2 cor28-2* mutant phenotype was most pronounced in R light, we focused on R light signalling in this study. Although a redundant function of COR27 and COR28 was already described for their role in flowering time regulation (Li *et al.*, 2016), we wanted to test whether the effects on hypocotyl growth inhibition rely on both *COR27* and *COR28*, or on only one of them. Therefore, we measured fluence rate response curves for hypocotyl growth in R light for the *cor27-2* and *cor28-2* single mutants (Figure S2a). Single mutations in either *COR27* or *COR28* had only a very weak effect on hypocotyl growth in R light, suggesting that COR27 and COR28 act redundantly in R light-dependent hypocotyl growth inhibition, similar to their redundant function in the regulation of flowering.

Both phyA and phyB interact with and potentially modulate light responses through COR27 and COR28. To investigate if the hypersensitivity to R light is phyA- or phyB-dependent, we generated *cor27-2 cor28-2 phyA-211* and *cor27-2 cor28-2 phyB-9* triple mutants and analysed hypocotyl growth of these lines under constant R light (Figure 2c; Figure S1). The introduction of the *cor27-2 cor28-2* double mutation into the *phyA-211* background led to reduced hypocotyl growth in R light compared with the *phyA-211* single mutant, whereas the *cor27-2 cor28-2 phyB-9* triple mutant was almost completely insensitive to R light, similar to the *phyB-9* single mutant. Thus, the hypersensitivity to R light of *cor27-2 cor28-2* requires phyB but does not depend on phyA (Figure 2c; Figure S1).

COR27 and COR28 protein abundance is regulated by R, FR, B and white light

COR27 and COR28 were previously described to be stabilized by B light (Li *et al.*, 2016), but the underlying molecular mechanism is still unclear and it is not known if other light qualities stabilize COR27 and COR28. We used seedlings expressing HA-YFP-tagged versions of COR27 and COR28 to investigate light regulation at the protein level. Expression of pCOR28:YFP-COR28 complements the *cor27-2 cor28-2* mutant phenotype and weak overexpression of HA-YFP-COR27 in Col-0 results in an opposite phenotype compared with the *cor27-2 cor28-2* mutant, suggesting that HA-YFP-COR27 and -COR28 are functional proteins (Figure S2b; Figure S3a). To avoid the effects of promoter activity on protein levels, we used Pro35S:HA-YFP-COR27 (COR27ox-1) and -COR28 expressing lines (COR28ox-1). We found that HA-YFP-COR27 and -COR28 accumulate in seedlings transferred from the dark to B, R, FR or white (W) light for 8 h (Figure 3a,b; Figures S4–S6).

COP1/SPA is involved in light regulation of COR27 and COR28 protein abundance

The COP1/SPA E3 ubiquitin ligase complex is a central component of light signalling in general and mediates protein degradation in response to light of different qualities. To test whether COP1/SPA complex activity affects the accumulation of COR27 and COR28 we crossed the COR27ox-1 line into *cop1-4* single and *spa1-100 spa2-2 spa3-1* (*spa123*) triple mutant backgrounds and COR28ox-1 into *cop1-4*. The proteome composition of dark-grown wildtype seedlings (i.e. etiolated seedlings) and mutants with a constitutively photomorphogenic phenotype such as *cop1-4* and *spa123* is different *per se* and therefore HA-YFP-COR27/-COR28 levels cannot be compared directly in the different genotypes. However, the difference between HA-YFP-COR27/-COR28 protein levels in dark-grown seedlings versus seedlings of the same genotype exposed to
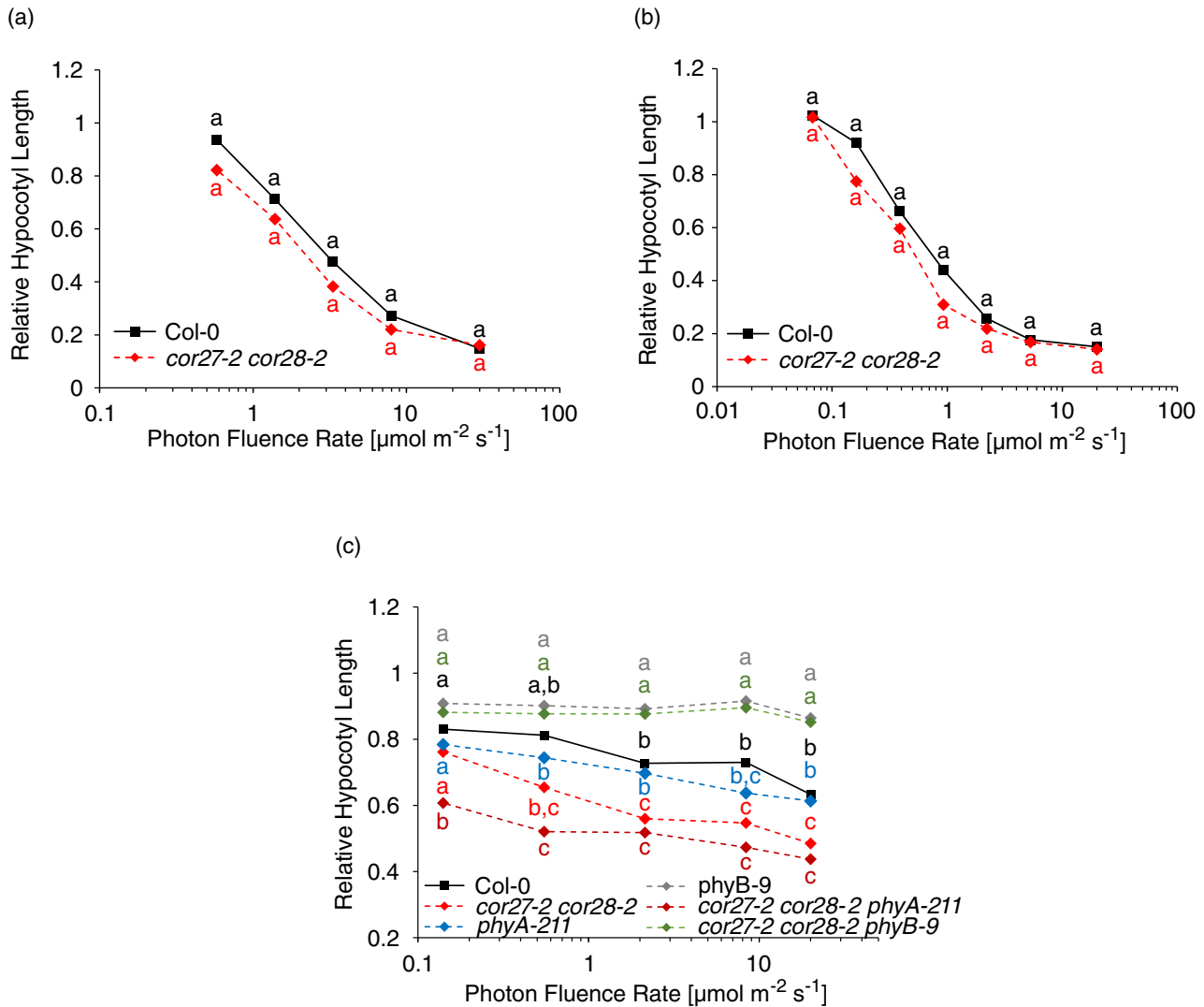
Figure 2. COR27 and COR28 are involved in phyB-dependent early seedling development.
(a–c) Fluence rate response curves for hypocotyl growth. Arabidopsis seedlings were grown for 4 days in continuous blue (a), far-red (b) or red (c) light. Mean hypocotyl length of seedlings grown in light relative to hypocotyl length of dark-grown seedlings is shown. $n = 3$ biological replicates; letters indicate levels of significance as determined by one-way ANOVA followed by *post hoc* Tukey's HSD test; $P < 0.05$.

light for 8 h is drastically reduced in *cop1-4* and *spa123* mutant background compared with the wildtype (Figure 3c,d; Figures S7 and S8), indicating that COP1 and SPA1/2/3 are involved in light regulation of HA-YFP-COR27 and HA-YFP-COR28 protein levels.

Inhibition of proteasome activity stabilizes COR27 and COR28 in the dark

Light has a much weaker effect on the increase of HA-YFP-COR27 and -COR28 levels in absence of functional COP1/SPA than in the wildtype background (Figure 3c,d). Therefore, we addressed the question whether this is due to a missing stabilization of COR27 and COR28 in light or a missing degradation of COR27 and COR28 in darkness that is repressed by light. We treated dark-grown COR27ox-1

and COR28ox-1 seedlings in wildtype, *cop1-4* and *spa123* background with the proteasome inhibitor Bortezomib (Kisselev *et al.*, 2012; Zhu and Huq, 2019). Treatment with Bortezomib lead to an increase of HA-YFP-COR27 and HA-YFP-COR28 abundance in the wildtype, but this effect was substantially reduced in the *cop1-4* and *spa123* background (Figure 3e,f; Figure S9). This suggests that COR27 and COR28 are degraded by the proteasome in darkness in the presence of the COP1/SPA complex and that reduced function of COP1/SPA prevents proteasomal degradation of COR27 and COR28.

COR27 and COR28 bind to the COP1/SPA complex

The COP1/SPA complex ubiquitinates target proteins in dark-grown seedlings and both repression of COP1/SPA
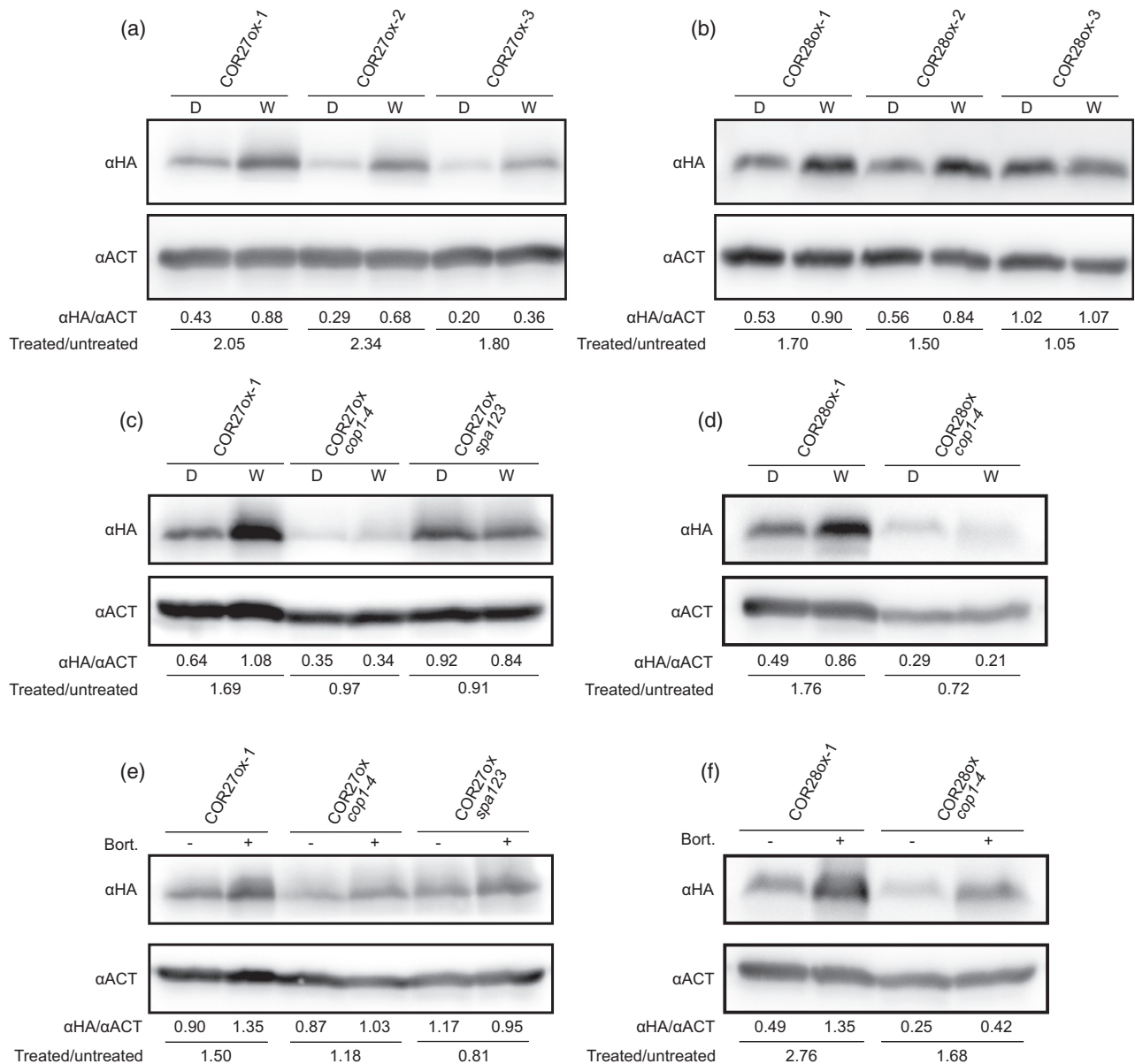
Figure 3. COR27 and COR28 protein stability is regulated by light and COP1/SPA.

(a,b) COR27 and COR28 are stabilized by light. Four-day-old, dark-grown seedlings of independent Arabidopsis lines expressing (a) Pro35S:HA-YFP-COR27 (COR27ox) and (b) Pro35S:HA-YFP-COR28 (COR28ox) were treated for 8 h with continuous white light (W, 70 μmol m^{-2} sec^{-1}) or darkness (D).

(c,d) COP1 and SPA1/2/3 control the accumulation of COR27 and COR28. Four-day-old, dark-grown seedlings of (c) COR27ox-1 in Col-0, *cop1-4* and *spa1-100 spa2-2 spa3-1* (*spa123*) background and (d) COR28ox-1 in Col-0 and *cop1-4* background were treated for 8 h with continuous W light (70 μmol m^{-2} sec^{-1}) or incubated in D conditions.

(e,f) Degradation of HA-YFP-COR27 and -COR28 in D conditions requires COP1 and SPAs. Four-day-old, dark-grown seedlings were submerged for 4 h in MS medium containing 40 μM Bortezomib or dimethyl sulphoxide (mock).

(a–f) Total protein was extracted and α-ACT and α-HA antibodies were used to detect endogenous actin and HA-YFP-COR27 and -COR28. 2× total protein was loaded for lines in *cop1-4* and *spa123* background. Western blots were quantified using ImageJ and α-HA signal relative to α-ACT signal and the ratio of treated to untreated sample is shown for each lane. Replicates shown in the figure are also included in Figures S5–S9. See Table S6 for statistical analysis.

activity by light-activated photoreceptors and light-dependent exclusion of COP1 from the nucleus lead to an accumulation of COP1/SPA target proteins in light (Hoecker, 2017; Podolec and Ulm, 2018). Consequently, we wanted to address the question whether COR27 and COR28 are

direct targets of the COP1/SPA complex. We analysed binding of COR27 and COR28 to COP1 and SPA1, and both COR27 and COR28 showed interaction with COP1 and SPA1 in a Y2H growth assay (Figure 4a). Furthermore, we could co-precipitate endogenous COP1 and SPA1 with HA-

1044   *Nikolai Kahle* et al.

YFP-COR27 and -COR28 in CoIP assays using COR27ox-1 and COR28ox-1 lines (Figure 4b), suggesting that they interact with COP1 and SPA1 *in planta*. The COP1 protein contains three structural motifs, a RING finger domain, involved in binding of E2 ubiquitin conjugates, a coiled-coil domain, responsible for the interaction with SPA1, and a
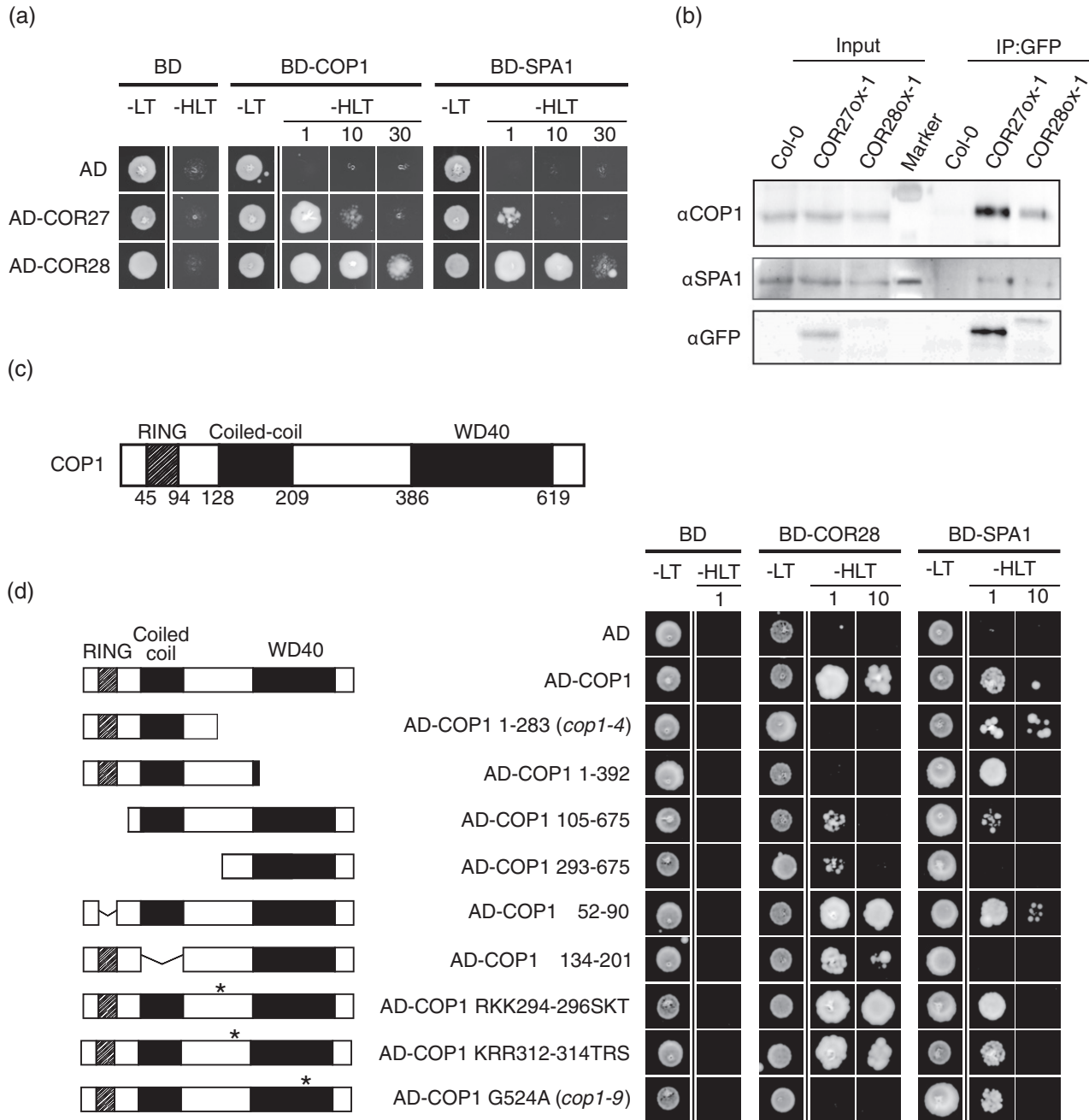

Figure 4. COR27 and COR28 interact with COP1 and SPA1.
(a) Yeast-two-hybrid growth assay. Yeast cultures (strain AH109) co-expressing either COR27 or COR28 fused to the GAL4-activation domain (AD) and COP1 or SPA1 fused to the GAL4-DNA-binding domain (BD) were grown on CSM -His -Leu -Trp (-HLT) plates containing 1, 10 or 30 mM 3-amino-1,2,4-triazole (1, 10, 30) to test for interaction.
(b) COP1 and SPA1 co-purify with COR27 and COR28. Native protein extracts of 3-day-old, dark-grown Arabidopsis seedlings expressing Pro35S:HA-YFP-COR27 (COR27ox-1) or Pro35S:HA-YFP-COR28 (COR28ox-1) were used for co-immunoprecipitation. Immunoprecipitation (IP) was performed using α-GFP-coupled magnetic beads. α-COP1 and α-SPA1 antibodies were used to detect endogenous COP1 and SPA1, and α-HA antibodies to detect HA-YFP-COR27 and -COR28.
(c) Schematic domain structure of COP1. Domains and positions of amino acid residues are indicated.
(d) COR28 interacts with the WD40 domain of COP1. Yeast-two-hybrid growth assay with COR28 and SPA1 fused to the GAL4-DNA-BD and truncated or mutated versions of COP1 fused to the GAL4-AD. Assay was performed as described in (a).

WD40 domain, which mediates the binding of substrates (Figure 4c) (Hoecker, 2017). Therefore, we used truncated versions of COP1 in a Y2H assay to identify the binding site of COR28 to COP1 (Figure 4d). While binding of COP1 and COR28 still occurred with a missing RING or coiled-coil domain, a truncated version of COP1 lacking the WD40 domain did not bind to COR28. However, binding of COP1 lacking the WD40 domain to SPA1 was retained, suggesting that this fragment is expressed and properly folded in yeast. Additionally, expression of the WD40 domain of COP1 alone was sufficient for interaction with COR28, indicating that COR28 binds to the WD40 domain of COP1. Taken together, our data suggest that COR27 and COR28 are direct targets of the COP1/SPA complex and degraded by the proteasome. This degradation is repressed by light-induced reduction of COP1/SPA activity, leading to accumulation of COR27 and COR28. Therefore, impaired COP1/SPA function in *cop1-4* and *spa123* mutants prevents the degradation of COR27 and COR28 in darkness (Figure 3c, d).

COR27 and COR28 bind to COP1 using a Val-Pro motif

Many proteins targeted for degradation by COP1 contain a Val-Pro (VP)-peptide motif essential for interaction with COP1 (Holm *et al.*, 2002; Uljon *et al.*, 2016; Lau *et al.*, 2019). It has been shown that COP1 directly binds the VP-peptide motifs of different light signalling components using its WD40 domain, and the human COP1 ortholog binds target proteins through a VP-peptide motif, suggesting a conserved mechanism of COP1 target recognition (Uljon *et al.*, 2016; Durzynska *et al.*, 2017; Lau *et al.*, 2019). We identified potential VP-peptide motifs in both COR27 and COR28 (Figures S10–S12), and substituted the respective VP pairs with two alanines (AA) (COR27 VP230-231AA and COR28 VP209-210AA) to test the relevance of the VP-peptide motifs of COR27 and COR28 for interaction with COP1. Indeed, substitution of the VP motif led to a complete loss of interaction with COP1 in yeast for both COR27 and COR28 (Figure 5a). In addition, binding to SPA1 was impaired as well (Figure 5a). In contrast, interaction with phyA and phyB was not affected, suggesting that COR27 VP230-231AA and COR28 VP209-210AA are properly folded and expressed in yeast (Figure S13). We then transformed Pro35S:HA-YFP-COR27 VP230-231AA and Pro35S:HA-YFP-COR28 VP209-210AA into the *cor27-2 cor28-2* double mutant (COR27 VP-AAox and COR28 VP-AAox) and used the resulting lines for CoIP experiments. In CoIP assays, we could co-precipitate much less endogenous COP1 with COR27 and COR28 containing a VP to AA substitution in the putative COP1 binding site than with wildtype COR27 and COR28, further indicating that COR27 and COR28 directly bind to the WD40 domain of COP1 via their VP-peptide motifs (Figure 5b). We then addressed the question whether binding to COP1 is indeed relevant for the

degradation of COR27 and COR28 in darkness. While the accumulation of wildtype COR27 and COR28 increased upon light irradiation, light did only weakly affect the abundance of COR27 and COR28 carrying a VP to AA substitution at the COP1 binding site (Figure 5c,d; Figures S5 and S6). In addition, transcript levels of *HA-YFP-COR27* and *HA-YFP-COR28* in COR27ox-1 and COR28ox-2 in darkness were higher compared with *HA-YFP-COR27 VP230-231AA* and *HA-YFP-COR28 VP209-210AA* expression levels in COR27 VP-AAox-1 and COR28 VP-AAox-2 (Figure S14), whereas the relative protein levels in these lines were similar (Figures S5 and S6). This is consistent with the notion that the degradation of COR27 VP230-231AA and COR28 VP209-210AA in darkness is reduced compared with wildtype COR27 and COR28. Therefore, we hypothesize that the COR27/28 VP-AAox lines partially mimic a light-grown accumulation pattern in darkness and the abundance of HA-YFP-COR27 VP230-231AA and HA-YFP-COR28 VP209-210AA is almost insensitive to light. The remaining light regulation of HA-YFP-COR27 VP230-231AA and HA-YFP-COR28 VP209-210AA protein abundance could be due to residual binding to COP1 (Figure 5b).

VP-AA mutant versions of COR27 and COR28 are strong inhibitors of phyB signalling

COR27 VP230-231AA and COR28 VP209-210AA did not show interaction with COP1 or SPA1 in Y2H experiments, but retained binding to phyA and phyB (Figure 5a,b; Figure S13). Thus, assuming that HA-YFP-COR27 VP230-231AA and HA-YFP-COR28 VP209-210AA still act on phyB signalling but escape from negative regulation by COP1/SPA, we hypothesized that COR27 VP-AAox and COR28 VP-AAox might show an opposite phenotype compared with the *cor27-2 cor28-2* mutant and be hyposensitive to light. Indeed, the COR27 VP-AAox and COR28 VP-AAox lines had longer hypocotyls than the wildtype in R light; COR27 VP-AAox seedlings were almost completely insensitive to R light, very similar to the *phyB-9* mutant. In contrast, strong overexpression of HA-YFP-COR27 and -COR28 in COR27ox-1 and COR28ox-1 lead to a hypersensitive response to R light (Figure 5e,f; Figures S1 and S3). However, moderate overexpression of HA-YFP-COR27 in COR27ox-3 resulted in increased hypocotyl elongation in R compared with the wildtype (Figures S1, S3 and S5), suggesting that strong overexpression of wildtype COR27 and COR28 might lead to antagonistic effects on COR27 and COR28 function. We speculate that this might be due to a competition of COR27/COR28 and positive factors of photomorphogenesis for binding to the COP1/SPA complex, resulting in partial stabilization of downstream targets of COP1/SPA in COR27ox-1 and COR28ox-1 but not in COR27ox-3. This is in line with the reduced hypocotyl growth of strong COR27 and COR28 overexpression lines grown in the dark (Figure S3). Consistent with our data,
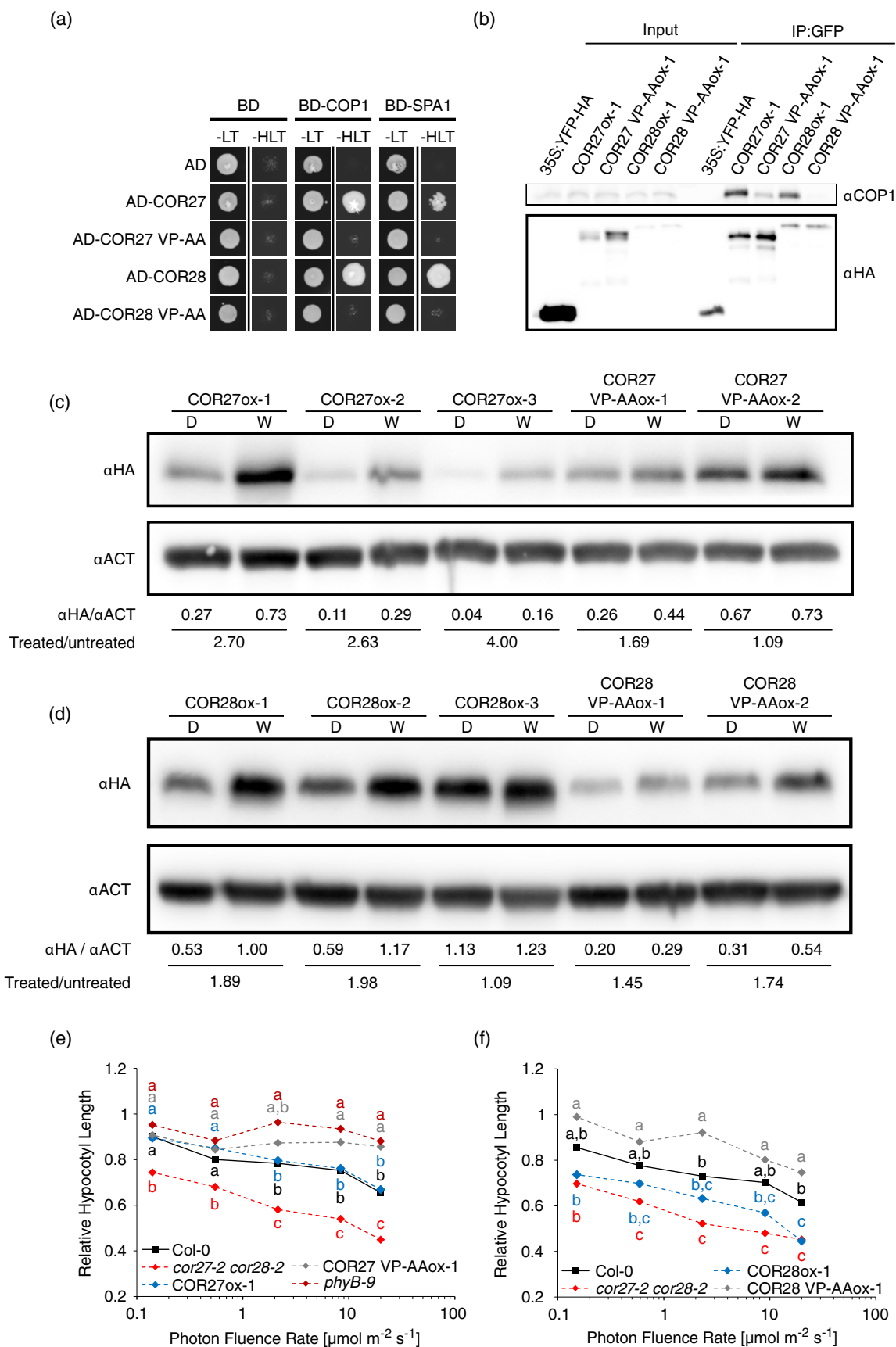
(a)

(b)

(c)

(d)

(e)

(f)

Figure 5. COR27 and COR28 bind to COP1 through a Val-Pro (VP) motif.
(a) Yeast-two-hybrid growth assay. Yeast cultures (strain AH109) co-expressing COR27, COR28 or point mutated versions of COR27 (COR27 VP-AA) or COR28 (COR28 VP-AA) fused to the GAL4-activation domain (AD) and COP1 or SPA1 fused to the GAL4-DNA-binding domain (BD) were grown on CSM -His -Leu -Trp (-HLT) plates containing 1 mM 3-amino-1,2,4-triazole to test for interaction.
(b) Binding of COP1 to COR27 VP-AA and COR28 VP-AA is reduced. Native protein extracts of 3-day-old, dark-grown Arabidopsis seedlings expressing Pro35S: HA-YFP-COR27 (COR27ox-1), Pro35S:HA-YFP-COR28 (COR28ox-1), Pro35S:HA-YFP-COR27 VP230-231AA (COR27 VP-AAox-1) or Pro35S:HA-YFP-COR28 VP209-210AA (COR28 VP-AAox-1) were used for co-immunoprecipitation. Immunoprecipitation (IP) was performed using α-GFP-coupled magnetic beads. α-COP1 and α-HA antibodies were used to detect endogenous COP1 and HA-tagged versions of COR27 and COR28.
(c,d) VP-peptide motif is required for light regulation of COR27 and COR28 protein stability. Four-day-old, dark-grown seedlings of independent COR27ox and COR27 VP-AAox (c) or COR28ox and COR28 VP-AAox lines (d) were treated for 8 h with continuous white light (W; 70 μmol m^{-2} sec^{-1}) or darkness (D). Total protein was extracted and α-ACT and α-HA antibodies were used to detect endogenous actin and HA-tagged versions of COR27 and COR28. Western blots were quantified using ImageJ and α-HA signal relative to α-ACT signal and the ratio of treated to untreated sample is shown for each lane. Replicates shown in the figure are also included in Figures S5 and S6. See Table S6 for statistical analysis.
(e,f) Fluence rate response curves for hypocotyl growth. Seedlings were grown for 4 days in continuous red light (cR). Mean hypocotyl length of seedlings grown in light relative to hypocotyl length of dark-grown seedlings is shown. n = 3 biological replicates; letters indicate levels of significance as determined by one-way ANOVA followed by *post hoc* Tukey's HSD test; $P < 0.05$.

this effect would be absent in lines expressing the COR27 and COR28 VP-AA mutant versions unable to bind COP1 (Figure S3). Overall, we conclude that VP-AA mutant versions of COR27 and COR28 are strong inhibitors of phyB signalling.

DISCUSSION

Previous work has shown that protein levels of COR27 and COR28 are low in etiolated seedlings and increase when seedlings are exposed to B light (Li *et al.*, 2016). However, the molecular mechanism underlying B light induced stabilization of COR27/COR28 and the function of COR27/COR28 in early seedling development remained unknown. Here, we show that COR27 and COR28 protein levels do not only increase upon treatment of seedlings with B light, but also when seedlings are exposed to R or FR light. Blocking the activity of the proteasome leads to enhanced accumulation of COR27 and COR28 in dark-grown seedlings, showing that COR27 and COR28 are targeted for degradation in the dark. The proteome composition of dark-grown wildtype seedlings, which are etiolated, and seedlings with a constitutively photomorphogenic phenotype such as *cop1-4* and *spa123* is different *per se* and therefore the effect of a short light treatment on the proteome of wildtype and *cop1-4* or *spa123* seedlings cannot be investigated by simply comparing protein levels in the wildtype and the mutant background. However, upon inhibition of proteasome activity, the relative increase in COR27 and COR28 protein abundance is much higher in dark-grown wildtype seedlings than in *cop1-4* and *spa123*, indicating that COR27/COR28 degradation is reduced in the absence of a functional COP1/SPA complex. Overall, we conclude that COP1 and SPA1/2/3 are involved in the destabilization of COR27/COR28 in etiolated seedlings, which however does not exclude that also other mechanisms could contribute to light regulation of COR27/COR28 protein stability. In agreement with the idea that COR27/COR28 are targets of COP1/SPA, COR27 and COR28 mutant versions impaired in binding COP1 and SPA1 are stabilized in dark-grown seedlings.

We found that lines strongly overexpressing HA-YFP-COR27 or -COR28 have shorter hypocotyls than the wild-type when grown in R light, that is, they have the same and not an opposite phenotype compared with the *cor27-2 cor28-2* double mutant. A similar observation has been reported by Li *et al.* (2016) who found that YFP-COR27 and GFP-COR28 overexpression lines are late flowering, similar to the *cor27-1* and *cor27-1 cor28-2* double mutant. However, expression of YFP-COR28 under the control of the endogenous COR28 promoter rescues the short hypocotyl phenotype of *cor27-2 cor28-2* and a line only weakly overexpressing HA-YFP-COR27 indeed has longer hypocotyls than the wildtype when grown in R light, that is, it has an opposite phenotype compared with the *cor27-2 cor28-2* double mutant. Thus, YFP-/GFP-tagged COR27/COR28 *per se* are functional proteins but strong overexpression appears to result in an antagonistic effect. With regard to this, it might be important to point out that strong COR27/ COR28 overexpression lines also have shorter hypocotyls than the wildtype when grown in the dark, while hypocotyl length of the weak COR27 overexpression line and the *cor27-2 cor28-2* mutant grown in the dark are indistinguishable from the wildtype. Furthermore, when grown in R light, lines strongly overexpressing COR27 VP-AA or COR28 VP-AA have longer hypocotyls than the wildtype, that is, they have an opposite phenotype compared with the *cor27-2 cor28-2* mutant, while hypocotyl length is indistinguishable from the wildtype in darkness. In conclusion, the negative effect on hypocotyl elongation of strong overexpression of wildtype COR27 and COR28 seems to be at least partially independent of light but dependent on their binding to COP1. This could either result from an independent, stabilizing or activating effect of COP1 on COR27/ COR28 or from strong overexpression of wildtype COR27 and COR28, which could partially block binding of other targets to COP1/SPA and thereby prevent their degradation and lead to reduced hypocotyl growth in the dark and in light. The latter would be similar to the mechanism for regulation of COP1/SPA employed by light-activated UVR8

and cryptochrome (CRY)2 (Ponnu *et al.*, 2019; Lau *et al.*, 2019). Overall, when overexpressed, COR27/COR28 might be substrates and regulators of COP1/SPA at the same time; however, the phenotype of weak COR27 overexpression lines suggests that the inhibitory effect of COR27/COR28 on COP1/SPA is possibly not relevant under wild-type conditions. Furthermore, the strong phenotype of COR27 VP-AA and COR28 VP-AA expressing lines indicates that blocking the VP-peptide binding site of COP1/SPA is unlikely to be the mechanism by which endogenous COR27 and COR28 regulate hypocotyl growth.

During early seedling development, plants are particularly vulnerable and tight regulation and integration of different signalling pathways is a prerequisite for survival. PhyB is a key factor for seedling establishment and allows seedlings emerging from the soil to adjust growth and development to the ambient environment. Hypocotyl growth in *cor27-2 cor28-2* is reduced compared with the wildtype, while *cor27-2 cor28-2 phyB-9* is indistinguishable from the *phyB-9* single mutant. Thus, in contrast to their function as positive regulators in flowering time control (Li *et al.*, 2016), COR27 and COR28 act as negative regulators in phyB-mediated photomorphogenesis, which might appear contradictory to the finding that COR27 and COR28 protein levels are increased in seedlings exposed to light. Most COP1/SPA targets involved in phyB signalling are

positive regulators of photomorphogenesis, such as ELON-GATED HYPOCOTYL 5 (HY5) and several members of the B-box domain transcription factor family (Gangappa and Botto, 2014; Xu, 2019). However, B-BOX DOMAIN PROTEIN 24 (BBX24)/SALT TOLERANCE (STO), BBX25/STO HOMO-LOG (STH) and BBX28 repress light signalling and are targets of COP1, similar to COR27 and COR28 (Indorf *et al.*, 2007; Gangappa *et al.*, 2013; Lin *et al.*, 2018). Light-induced stabilization of negative regulators of light signalling might be important to avoid overactivation of downstream signalling pathways and prevent an exaggerated response to light. BBX proteins primarily act through promoting or inhibiting HY5-dependent downstream signalling (Xu, 2019). Whether HY5 also plays a role downstream of COR27 and/or COR28 is unknown. COR27 and COR28 bind to chromatin of *TIMING OF CAB EXPRESSION 1* (*TOC1*)/ *PSEUDO-RESPONSE REGULATOR 1* (*PRR1*) and *PRR5*, and repress their expression (Li *et al.*, 2016). In addition to their clock-related phenotype, *toc1* and *prr5* mutants are also hyposensitive to R light with regard to inhibition of hypocotyl growth (Eriksson *et al.*, 2003; Más *et al.*, 2003; Yamamoto *et al.*, 2003; Nakamichi *et al.*, 2005). Hypocotyl growth in *toc1* and *prr5* has been measured in continuous R light without previous entrainment of the clock and therefore the hypocotyl growth phenotype under these conditions cannot be attributed to clock-related defects in
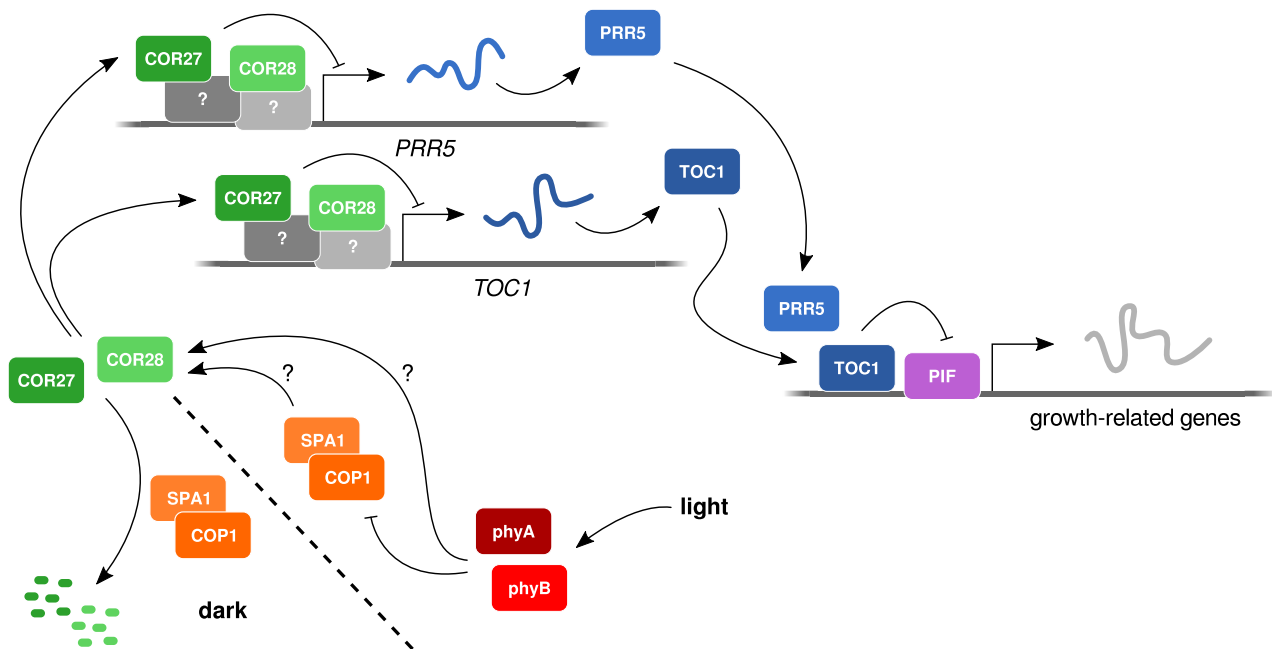

Figure 6. Hypothetical model for COR27/COR28 action.
Light-activated phytochromes repress the E3 ubiquitin ligase activity of COP1/SPA and promote the accumulation of COR27 and COR28. COR27/COR28 associate with the promoters of *TOC1* and *PRR5* and repress their expression (Li *et al.*, 2016). High levels of TOC1 and PRR5 antagonize PHYTOCHROME INTERACTING FACTORs (PIFs) and thereby repress hypocotyl growth (Yamamoto *et al.*, 2003; Más *et al.*, 2003; Nakamichi *et al.*, 2005; Martín *et al.*, 2018). If interaction of phytochromes and COR27/COR28 has an effect on light regulation of COP1/SPA-mediated COR27/COR28 turnover is still unknown. We show that COR27/COR28 are destabilized by COP1/SPA in the dark but we cannot exclude that COP1/SPA could have a positive effect on COR27/COR28 protein stability in light.

toc1 and *prr5* (Eriksson *et al.*, 2003; Más *et al.*, 2003; Yamamoto *et al.*, 2003; Nakamichi *et al.*, 2005). Thus, *TOC1* and *PRR5* might be the targets of COR27 and COR28 in the regulation of hypocotyl growth. Stabilization of COR27/COR28 in light could lead to the repression of *TOC1* and *PRR5* and thereby promote hypocotyl growth; in contrast, in the *cor27-2 cor28-2* mutant, *TOC1* and *PRR5* expression would be increased, possibly leading to suppression of hypocotyl growth (Figure 6). TOC1, PRR5 and other PRRs antagonize the growth-promoting function of PIFs during the light phase in seedlings grown in day/night cycles (Martín *et al.*, 2018; Li *et al.*, 2020). Thus, regulation of hypocotyl growth by COR27/COR28 might indirectly, through TOC1 and PRR5, also involve PIFs.

Proteins with similarity to COR27/COR28 can be identified in various land plant species as well as in the charophyte alga *Chara braunii*. The overall amino acid identity of COR27/COR28 and potential COR27/COR28 homologues is comparably low, i.e. in the range of 20–30%, but conserved motifs (MEME-1 to -5) can be identified using the MEME SUITE software package (Figures S10–S12). These motifs are present in all or most potential COR27/COR28 homologues, including sequences from *Selaginella moellendorffii*, *Physcomitrella patens*, *Marchantia polymorpha* and *Chara braunii*, and they are linked by regions of very low sequence similarity, which are considerably longer in potential COR27/COR28 homologues from non-vascular plants (Chara, Marchantia, Physcomitrella) than vascular plants. The MEME-5 motif contains the VP-peptide motif required for COP1/SPA-mediated regulation of COR27/COR28 protein stability in Arabidopsis, suggesting that binding of COP1 and possibly regulation of protein turnover by COP1 might be ancestral properties of COR27/COR28. Similar to MEME-5, MEME-1 is also present in potential COR27/COR28 homologues from Chara, Physcomitrella and Selaginella, and might serve an ancestral function; however, in contrast to MEME-5, the function of MEME-1 is still unknown. In the course of evolution of land plants, COR27/COR28 might have acquired additional motifs, such as MEME-2, -3 and -4, which might extend the function of COR27/COR28 and/or put them under the control of specific signalling pathways. COR27/COR28 bind to chromatin but in contrast to transcription factors they do not contain *bona fide* DNA-binding sites (Li *et al.*, 2016). MEME motifs, for example, could be involved in DNA binding and/or interaction with proteins associated with DNA.

We identified COR27 and COR28 as phyA- and phyB-interacting proteins and can show that they play a role in phytochrome signalling. However, we still do not know if the interaction *per se* is of functional relevance and, if it is, how it contributes to phytochrome signalling through COR27/COR28. Binding of phytochromes might play a role in the regulation of COP1/SPA-dependent control of COR27/COR28 protein stability. In another hypothetical

scenario, COR27/COR28 could recruit phytochromes into specific complexes with a function in light signalling. For instance, phytochromes associate with numerous promoters but how they bind chromatin and how this binding affects gene expression is still unclear (Legris *et al.*, 2019). COR27/COR28 have been shown to bind chromatin of target genes and a hypothetical function could be to recruit phytochromes to the promoter of these genes to put them under light control.

Here, we focused on the function of COR27 and COR28 in phyB-mediated R light signalling, but physiological and biochemical data presented in this study suggest that COR27 and COR28 also play a role in downstream signalling of phyA and one or several B light receptors. The function of COR27 and COR28 in B light could depend on phyA but also a requirement or contribution of CRY1 and/or CRY2 is possible.

Overall, we have shown that COR27 and COR28 play a role in R light signalling downstream of phyB and are regulated by the COP1/SPA E3 ubiquitin ligase complex. In future work it will be important to investigate what molecular mechanism links COR27/COR28 to the regulation of gene expression and to elucidate a potential function of photoreceptors in this process. Given that COR27/COR28 are regulated by light, the circadian clock and temperature, they are promising candidates for the integration of these signalling pathways, which is key for survival under diverse and rapidly changing environments.

EXPERIMENTAL PROCEDURES

Cloning of plasmid constructs

Plasmid constructs used in this study were generated as described in Tables S1 and S2. All plasmid constructs have been verified by sequencing. *COR28* in the plasmid construct pPPO70HA-COR28 still contains the last intron in *COR28*, which is spliced in the At4g33980.1 splicing variant but retained in At4g33980.2. This affects neither the HA-YFP tag, which is fused to the N-terminus, nor any of the MEME motifs (Figures S11 and S12). The splicing variants differ by 14 amino acids (At4g33980.1: 218 aa; At4g33980.2: 232 aa) and possibly run as one band on sodium dodecyl sulphate–polyacrylamide gel electrophoresis (SDS-PAGE) gels.

Plant material and growth conditions

All *A. thaliana* lines used in this study were in Col-0 background. *Cop1-4*, *spa1-100 spa2-2 spa3-1* (*spa123*), *phyA-211*, *phyB-9* and ProPhyB:phyB-mCer *phyB-9* (PHYB-mCer) have been described previously (Reed *et al.*, 1993; Reed *et al.*, 1994; McNellis *et al.*, 1994; Ordóñez-Herrera *et al.*, 2015; Li *et al.*, 2016; Enderle *et al.*, 2017). *cor27-2* (SALK_042072, N668138) and *cor28-2* (SALK_137155, N664112) were obtained from the Nottingham Arabidopsis Stock Centre (Alonso *et al.*, 2003) and have been described previously (Li *et al.*, 2016). ProCOR28:YFP-COR28 *cor27-2 cor28-2*, COR27ox, COR27 VP-AAox, COR28ox and COR28 VP-AAox lines were generated using the *Agrobacterium tumefaciens* floral dip transformation method (Clough and Bent, 1998; Davis *et al.*, 2009). For ProCOR28:YFP-COR28 *cor27-2 cor28-2* lines, pCHF-pCOR28-YFP-COR28 (T-DNA vector containing

ProCOR28:YFP-COR28:TerRbcS; resistance to Basta as the selection marker) was transformed into *cor27-2 cor28*-2. For COR27ox and COR28ox, pPPO70v1HA-COR27 and pPPO70v1HA-COR28 (T-DNA vectors containing Pro35S:HA-YFP-COR27/COR28:TerRbcS; resistance to Butafenacil/Inspire as the selection marker) were transformed into Col-0. For COR27 VP-AAox and COR28 VP-AAox, pCHF70HA-COR27 VP230-231AA and pCHF70HA-COR28 VP209-210AA (T-DNA vectors containing Pro35S:HA-YFP-COR27 VP230-231AA/COR28 VP209-210AA:TerRbcS; resistance to Basta as the selection marker) were transformed into *cor27-2 cor28-2*. All additional mutant combinations used in this study were obtained by crossing of the above-mentioned lines. COR27ox-1 and COR28ox-1 were used for crossing COR27ox and COR28ox in different backgrounds. Genotyping was performed as described in Tables S3 and S4.

All experiments were performed using seedlings grown on four layers of filter paper (Macherey-Nagel; cat. no: MN615) soaked with sterile water. Seeds were stratified for 2–4 days at 4°C in darkness and germination was induced by incubation in W light (70 μmol m^{-2} sec^{-1}) for 8 h at 22°C. After an additional 12 h in darkness at 22°C, seedlings were transferred to the indicated light conditions at 22°C.

Measurement of hypocotyl

Seedlings were grown in continuous light at the indicated photon fluence rates and hypocotyl lengths of at least 20 individual seedlings per replicate were measured on the fourth day after germination induction using ImageJ (Schneider *et al.*, 2012). Figures show mean hypocotyl length of three biological replicates.

Protein extraction and immunoblotting

Seedlings were grown for 4 days in darkness and treated as described in the figure legends. Total protein was extracted using preheated (95°C) extraction buffer (4 M urea, 65 mM Tris/HCl pH 7.3, 3% SDS, 10% glycerol, 0.05% bromophenol blue, 10 mM dithiothreitol). Total protein extracts were separated by 10% SDS-PAGE and transferred to polyvinylidene fluoride membranes. Membranes were probed with α-HA (BioLegend, San Diego, CA, USA; cat. no. 901502, monoclonal, mouse, 16B12, dilution 1:2000), α-phyB (monoclonal, mouse, B6-B3, dilution 1:250), α-COP1 (polyclonal, rabbit, dilution 1:250), α-SPA1 (polyclonal, rabbit, dilution 1:250), α-phyA (Agrisera, Vännäs, Sweden; cat. no. AS07 220, polyclonal, rabbit, dilution 1:1500) and α-actin (Sigma-Aldrich, St. Louis, MO, USA; cat. no. A0480, monoclonal, mouse, 1:3000 dilution) (Hirschfeld *et al.*, 1998; Balcerowicz *et al.*, 2011). Immunodetections were performed using alkaline phosphatase horse antimouse IgG antibody (Vector Laboratories, Burlingame, CA, USA; cat. no. AP-2000, 1:10 000 dilution) with CDP-Star (Sigma-Aldrich; cat. no. 11759051001) or either horseradish peroxidase conjugated goat antirabbit IgG (H&L) (Agrisera; cat. no. AS09 602, dilution 1:20 000) or rabbit antimouse IgG (whole molecule)-peroxidase antibody (Sigma-Aldrich; cat. no. A9044, dilution 1:20 000) with Amersham ECL Prime Western Blotting Detection Reagent (GE Healthcare, Chicago, IL, USA; cat. no. RPN2232). For stripping, membranes were incubated in stripping buffer (62.5 mM Tris/HCl pH 6.8, 2% SDS, 100 mM 2-mercaptoethanol) for 30 min at 60°C. Blots were quantified as described in Enderle *et al.* (2017) using ImageJ.

CoIP

Seedlings were grown for 4 days in darkness. All CoIP experiments were performed in green light. Protein was extracted using IP buffer [100 mM NaPO$_4$ pH 7.8, 150 mM NaCl, 1 mM KCl, 1 mM EDTA, 1% PEG 4000, 0.5% Triton X-100, 1 mM Na$_3$OV$_4$, 2 mM

Na$_4$P$_2$O$_7$, 10 mM NaF, 1× Protease inhibitor Cocktail (Sigma-Aldrich; cat. no. I3911), 1× complete protease inhibitor cocktail (Sigma-Aldrich; cat. no. 04693159001)]. For phyA interaction, protein extracts received a 5-min light pulse either with R (680 nm) or FR light (780 nm). For phyB interaction, plants were treated either with 2 h of R light (660 nm, 20 μmol m^{-2} sec^{-1}) or with 2 h of R light (660 nm, 20 μmol m^{-2} sec^{-1}) followed by 5 min of FR light (760 nm, 20 μmol m^{-2} sec^{-1}) before harvesting. Fifty-microlitres of Anti-GFP MicroBeads (Miltenyi Biotec, Bergisch Gladbach, Germany; cat. no. 130-091-125) or Anti-HA MicroBeads (Miltenyi Biotec; cat. no. 130-091-122) was then added to the extracts. Following 2 h of incubation in darkness, beads were washed thoroughly with IP buffer and elution was performed using preheated (95°C) elution buffer (100 mM Tris/HCl pH 6.8, 4% SDS, 20% glycerol, 0.05% bromophenol blue). Elutions were analysed by SDS-PAGE and immunoblotting.

Y2H screen

The Y2H screen for phyA-interacting proteins was done as previously described (Sheerin *et al.*, 2015).

Y2H growth assay

Y2H plasmids were co-transformed into *Saccharomyces cerevisiae* strain AH109 (Clontech, 2009) using a Frozen-EZ Yeast Transformation Kit (Zymo Research, Freiburg, Germany; cat. no. T2001). Transformants were isolated by selective growth medium lacking leucine and tryptophan. Transformed yeast was suspended in sterile water, diluted to an OD$_{600}$ = 0.1 and 5 μl was spotted on to growth medium containing indicated concentrations of 3-amino-1,2,4-triazole and lacking leucine, tryptophan and histidine. For Y2H assays with phytochromes, 20 μM phycocyanobilin (Livchem Logistics, Frankfurt, Germany; cat. no. FSIP14137) was added to the media. Plates were incubated for 7 days at 26°C in either darkness, R light (2 μmol m^{-2} sec^{-1}) or FR light (10 μmol m^{-2} sec^{-1}).

M2H assay

The split transcription factor system for light controlled gene expression in eukaryotic cells was based on a previously reported setup (Müller *et al.*, 2013; Müller *et al.*, 2014; Golonka *et al.*, 2019). For testing of COR27 and COR28, *At*PIF6 (1–100) was replaced by the corresponding coding sequences by AQUA cloning (Beyer *et al.*, 2015). Chinese hamster ovary cells (CHO-K1; DSMZ, Braunschweig, Germany) were cultivated in HAM's F12 medium (PAN Biotech, Aidenbach, Germany; no. P04-14500) supplemented with 10% (v/v) tetracycline-free fetal bovine serum (PAN Biotech; no. P30-3602; batch no. P080317TC) and 1.4% (v/v) streptomycin (PAN Biotech; no. P06-07100). CHO-K1 cells (5 × 10^4) were transfected using polyethylenimine (PEI; Polysciences Inc. Europe, Hirschberg, Germany; no. 23966-1) (Baaske *et al.*, 2018; Golonka *et al.*, 2019). DNA (0.75 μg) was diluted in 50 μl OptiMEM (Invitrogen, Thermo Fisher Scientific, Waltham, MA, USA) and mixed with a PEI/OptiMEM mix (2.5 μl PEI solution in 50 μl OptiMEM). The DNA-PEI mix was added to the cells after 15 min of incubation at room temperature. At 4 h post-transfection, the medium was exchanged. CHO-K1 cells were transfected with the reporter plasmid tetO$_{13}$-CMVmin-SEAP-BGH-SV40-Gaussia (pPF034) and the different *At*PhyA or B with potential interactors. All plasmids were transfected in equal amounts (w/w). At 24 h post-transfection, the cells were supplemented with 15 μM phycocyanobilin (24 mM stock solution in dimethyl sulphoxide; Frontier Scientific, Logan, UT, USA; no. P14137) and incubated for 1 h. The cells were then illuminated with 660 nm light for 24 h at an intensity of 20 μmol m^{-2} sec^{-1} or kept in darkness. As a negative control, the

reporter construct alone was transfected. As positive controls, known interaction pairs were transfected (PhyA/FHL; PhyB/PIF6). Exchange of media and other cell-handling was done under 522 nm safe light, to prevent inadvertent activation of the light-sensitive systems (Baaske *et al.*, 2018; Golonka *et al.*, 2019).

For SEAP activity measurement, the supernatant of transfected cells was transferred to 96-well round-bottom microtitre plates and incubated at 68°C for 1 h to inactivate endogenous phosphatases. Afterwards, 80 μl of the supernatant was transferred to a 96-well flat-bottom microtitre plates, and per well 100 μl SEAP buffer (20 mM homoarginine, 1 mM MgCl$_2$, 21% (v/v) diethanolamine) was added (Baaske *et al.*, 2018; Golonka *et al.*, 2019). After addition of 20 μl 120 mM para-nitrophenyl phosphate, the absorption at 405 nm was measured for 1 h using a BMG Labtech CLARIOstar or a TriStar2 S LB 942 multimode plate reader (Berthold Technologies, Bad Wildbad, Germany) (Baaske *et al.*, 2018; Golonka *et al.*, 2019). Outliers were statistically determined and excluded (Jacobs and Dinman, 2004).

Identification of homologues and sequence alignment

Potential homologues were identified using Protein BLAST from the National Center for Biotechnology Information (NCBI) and Uni-Prot. We used the annotated protein sequences of COR27 and COR28 from The Arabidopsis Information Resource (TAIR) as query sequences. Based on maximum score and percentage identity we chose potential homologues (Data S1) and compiled a protein alignment using the ClustalO Alignment Tool from JALVIEW (V 2.11.0) with default settings (Waterhouse *et al.*, 2009; Sievers *et al.*, 2011). In addition, we submitted the sequences of potential COR27/COR28 homologues to MEME (http://meme-suite.org/; default settings were used) to search for conserved motifs (Bailey *et al.*, 2009). All sequences from Data S1 were used for the motif search, while sequences from Physcomitrella, Marchantia and Chara were omitted for the sequence alignment to avoid long gaps.

RNA extraction and transcription analysis

Quantification of transcript levels was performed as described in Enderle *et al.*, 2017. Quantitative reverse transcription–polymerase chain reaction was performed using a SensiFAST™ SYBR Hi-ROX Kit (Bioline Medidian Bioscience, London, UK; cat. no. BIO-92005) and primers specific for *YFP* and *ACT1* (Table S5).

Statistical analysis

ANOVA and *post hoc* Tukey's HSD tests were performed for statistical analysis.

ACCESSION NUMBERS

COP1, At2g32950; *COR27*, At5g42900; *COR28*, At4g33980; *PHYA*, At1g09570; *PHYB*, At2g18790; and *SPA1*, At2g46340.

AUTHOR CONTRIBUTIONS

NK, DJS, MDZ, and AH conceptualized research. NK, DJS, RR, PF, LAK, PS, and DL carried out the investigation. KK and UH provided resources. Visualization was done by NK, PF, and LAK. NK, MDZ, and AH wrote the original draft of the manuscript. NK, DJS, PS, DL, MDZ, UH, and AH commented on the draft version of the manuscript. All authors reviewed the final version of the manuscript. Project administration was carried out by AH. Funding was acquired by AH, NK, MDZ, and UH.

CONFLICT OF INTERESTS

The authors declare that they have no competing interests.

DATA AVAILABILITY STATEMENT

All relevant data can be found within the manuscript and its supporting materials.

SUPPORTING INFORMATION

Additional Supporting Information may be found in the online version of this article.

Figure S1. Phenotype of seedlings grown in darkness or in red light.
Figure S2. Hypocotyl length of *cor27-2* and *cor28-2* single mutants and *cor28-2* complementation lines.
Figure S3. COR27 and COR28 affect red light-dependent hypocotyl growth inhibition.
Figure S4. Accumulation of COR27 and COR28 in red (R), far-red (FR) and blue light (B).
Figure S5. Western blot triplicate showing accumulation of COR27 in light.
Figure S6. Western blot triplicate showing accumulation of COR28 in light.
Figure S7. Western blot triplicate showing accumulation of COR27 in *cop1-4* and *spa123*.
Figure S8. Western blot triplicate showing accumulation of COR28 in *cop1-4*.
Figure S9. Western blot triplicate showing accumulation of COR27 in response to Bortezomib.
Figure S10. Sequence alignment for potential COR27 and COR28 homologues.

REFERENCES

Alonso, J.M., Stepanova, A.N., Leisse, T.J. *et al*. (2003) Genome-wide insertional mutagenesis of *Arabidopsis thaliana*. *Science*, **301**, 653–657.

Al-Sady, B., Ni, W., Kircher, S., Schäfer, E. and Quail, P.H. (2006) Photoactivated phytochrome induces rapid PIF3 phosphorylation prior to proteasome-mediated degradation. *Mol. Cell*, **23**, 439–446.

Baaske, J., Gonschorek, P., Engesser, R. *et al*. (2018) Dual-controlled optogenetic system for the rapid down-regulation of protein levels in mammalian cells. *Sci. Rep.* **8**, 15024.

Bailey, T.L., Boden, M., Buske, F.A., Frith, M., Grant, C.E., Clementi, L., Ren, J., Li, W.W. and Noble, W.S. (2009) MEME SUITE: tools for motif discovery and searching. *Nucleic Acids Res.* **37**, W202–W208.

Balcerowicz, M., Fittinghoff, K., Wirthmueller, L., Maier, A., Fackendahl, P., Fiene, G., Koncz, C. and Hoecker, U. (2011) Light exposure of Arabidopsis seedlings causes rapid de-stabilization as well as selective post-translational inactivation of the repressor of photomorphogenesis SPA2. *Plant J.* **65**, 712–723.

Balcerowicz, M., Kerner, K., Schenkel, C. and Hoecker, U. (2017) SPA proteins affect the subcellular localization of COP1 in the COP1/SPA ubiquitin ligase complex during photomorphogenesis. *Plant Physiol.* **174**, 1314–1321.

Bauer, D., Viczián, A., Kircher, S. *et al*. (2004) CONSTITUTIVE PHOTOMORPHOGENESIS 1 and multiple photoreceptors control degradation of PHYTOCHROME INTERACTING FACTOR 3, a transcription factor required for light signaling in Arabidopsis. *Plant Cell*, **16**, 1433–1445.

Beyer, H.M., Gonschorek, P., Samodelov, S.L., Meier, M., Weber, W. and Zurbriggen, M.D. (2015) AQUA cloning: a versatile and simple enzyme-free cloning approach. *PLoS One*, **10**, e0137652.

Clontech. (2009) *Yeast Protocols Handbook*. Mountain View: Clontech Laboratories.

Clough, S.J. and Bent, A.F. (1998) Floral dip: a simplified method for *Agrobacterium*-mediated transformation of *Arabidopsis thaliana*. *Plant J.* **16**, 735–743.

Davis, A.M., Hall, A., Millar, A.J., Darrah, C. and Davis, S.J. (2009) Protocol: streamlined sub-protocols for floral-dip transformation and selection of transformants in *Arabidopsis thaliana*. *Plant Methods*, **5**, 3.

Durzynska, I., Xu, X., Adelmant, G., Ficarro, S.B., Marto, J.A., Sliz, P., Uljon, S. and Blacklow, S.C. (2017) STK40 is a pseudokinase that binds the E3 ubiquitin ligase COP1. *Structure*, **25**, 287–294.

Enderle, B., Sheerin, D.J., Paik, I., Kathare, P.K., Schwenk, P., Klose, C., Ulbrich, M.H., Huq, E. and Hiltbrunner, A. (2017) PCH1 and PCHL promote photomorphogenesis in plants by controlling phytochrome B dark reversion. *Nat. Commun.* **8**, 2221.

Eriksson, M.E., Hanano, S., Southern, M.M., Hall, A. and Millar, A.J. (2003) Response regulator homologues have complementary, light-dependent functions in the Arabidopsis circadian clock. *Planta*, **218**, 159–162.

Gangappa, S.N. and Botto, J.F. (2014) The BBX family of plant transcription factors. *Trends Plant Sci.* **19**, 460–470.

Gangappa, S.N., Crocco, C.D., Johansson, H., Datta, S., Hettiarachchi, C., Holm, M. and Botto, J.F. (2013) The *Arabidopsis* B-BOX protein BBX25 interacts with HY5, negatively regulating *BBX22* expression to suppress seedling photomorphogenesis. *Plant Cell*, **25**, 1243–1257.

Golonka, D., Fischbach, P., Jena, S.G., Kleeberg, J.R.W., Essen, L.-O., Toettcher, J.E., Zurbriggen, M.D. and Möglich, A. (2019) Deconstructing and repurposing the light-regulated interplay between *Arabidopsis* phytochromes and interacting factors. *Commun. Biol.* **2**, 448.

Hirschfeld, M., Tepperman, J.M., Clack, T., Quail, P.H. and Sharrock, R.A. (1998) Coordination of phytochrome levels in *phyB* mutants of Arabidopsis as revealed by apoprotein-specific monoclonal antibodies. *Genetics*, **149**, 523–535.

Hoecker, U. (2005) Regulated proteolysis in light signaling. *Curr. Opin. Plant Biol.* **8**, 469–476.

Hoecker, U. (2017) The activities of the E3 ubiquitin ligase COP1/SPA, a key repressor in light signaling. *Curr. Opin. Plant Biol.* **37**, 63–69.

Holm, M., Ma, L.-G., Qu, L.-J. and Deng, X.-W. (2002) Two interacting bZIP proteins are direct targets of COP1-mediated control of light-dependent gene expression in *Arabidopsis*. *Genes Dev.* **16**, 1247–1259.

Indorf, M., Cordero, J., Neuhaus, G. and Rodríguez-Franco, M. (2007) SALT TOLERANCE (STO), a stress-related protein, has a major role in light signalling. *Plant J.* **51**, 563–574.

Jacobs, J.L. and Dinman, J.D. (2004) Systematic analysis of bicistronic reporter assay data. *Nucleic Acids Res.* **32**, e160.

Jang, I.-C., Henriques, R., Seo, H.S., Nagatani, A. and Chua, N.-H. (2010) *Arabidopsis* PHYTOCHROME INTERACTING FACTOR proteins promote phytochrome B polyubiquitination by COP1 E3 ligase in the nucleus. *Plant Cell*, **22**, 2370–2383.

Jang, I.-C., Yang, J.-Y., Seo, H.S. and Chua, N.-H. (2005) HFR1 is targeted by COP1 E3 ligase for post-translational proteolysis during phytochrome A signaling. *Genes Dev.* **19**, 593–602.

Jang, K., Gil Lee, H., Jung, S.-J., Paek, N.-C. and Joon Seo, P. (2015) The E3 ubiquitin ligase COP1 regulates thermosensory flowering by triggering GI degradation in *Arabidopsis*. *Sci. Rep.* **5**, 12071.

Kami, C., Lorrain, S., Hornitschek, P. and Fankhauser, C. (2010) Light-regulated plant growth and development. *Curr. Top. Dev. Biol.* **91**, 29–66.

Kisselev, A.F., van der Linden, W.A. and Overkleeft, H.S. (2012) Proteasome inhibitors: an expanding army attacking a unique target. *Chem. Biol.* **19**, 99–115.

Lau, K., Podolec, R., Chappuis, R., Ulm, R. and Hothorn, M. (2019) Plant photoreceptors and their signaling components compete for COP1 binding via VP peptide motifs. *EMBO J.* **38**, e102140.

Lau, O.S. and Deng, X.W. (2012) The photomorphogenic repressors COP1 and DET1: 20 years later. *Trends Plant Sci.* **17**, 584–593.

Laubinger, S., Fittinghoff, K. and Hoecker, U. (2004) The SPA quartet: a family of WD-repeat proteins with a central role in suppression of photomorphogenesis in Arabidopsis. *Plant Cell*, **16**, 2293–2306.

Lee, N. and Choi, G. (2017) Phytochrome-interacting factor from *Arabidopsis* to liverwort. *Curr. Opin. Plant Biol.* **35**, 54–60.

Legris, M., Ince, Y.Ç. and Fankhauser, C. (2019) Molecular mechanisms underlying phytochrome-controlled morphogenesis in plants. *Nat. Commun.* **10**, 5219.

Li, N., Zhang, Y., He, Y., Wang, Y. and Wang, L. (2020) Pseudo response regulators regulate photoperiodic hypocotyl growth by repressing PIF4/5 transcription. *Plant Physiol.* **183**, 686–699.

Li, X., Ma, D., Lu, S.X., Hu, X., Huang, R., Liang, T., Xu, T., Tobin, E.M. and Liu, H. (2016) Blue light- and low temperature-regulated COR27 and COR28 play roles in the Arabidopsis circadian clock. *Plant Cell*, **28**, 2755–2769.

Lin, F., Jiang, Y., Li, J., Yan, T., Fan, L., Liang, J., Chen, Z.J., Xu, D. and Deng, X.W. (2018) B-BOX DOMAIN PROTEIN28 negatively regulates photomorphogenesis by repressing the activity of transcription factor HY5 and undergoes COP1-mediated degradation. *Plant Cell*, **30**, 2006–2019.

Lu, X.-D., Zhou, C.-M., Xu, P.-B., Luo, Q., Lian, H.-L. and Yang, H.-Q. (2015) Red-light-dependent interaction of phyB with SPA1 promotes COP1–SPA1 dissociation and photomorphogenic development in *Arabidopsis*. *Mol. Plant*, **8**, 467–478.

Martín, G., Rovira, A., Veciana, N. *et al*. (2018) Circadian waves of transcriptional repression shape PIF-regulated photoperiod-responsive growth in *Arabidopsis*. *Curr. Biol.* **28**, 311–318.e5.

Más, P., Alabadí, D., Yanovsky, M.J., Oyama, T. and Kay, S.A. (2003) Dual role of TOC1 in the control of circadian and photomorphogenic responses in Arabidopsis. *Plant Cell*, **15**, 223–236.

McNellis, T.W., von Arnim, A.G., Araki, T., Komeda, Y., Miséra, S. and Deng, X.W. (1994) Genetic and molecular analysis of an allelic series of *cop1*

mutants suggests functional roles for the multiple protein domains. *Plant Cell*, **6**, 487–500.

Mikkelsen, M.D. and Thomashow, M.F. (2009) A role for circadian evening elements in cold-regulated gene expression in Arabidopsis. *Plant J.* **60**, 328–339.

Müller, K., Engesser, R., Timmer, J., Nagy, F., Zurbriggen, M.D. and Weber, W. (2013) Synthesis of phycocyanobilin in mammalian cells. *Chem. Commun.* **49**, 8970–8972.

Müller, K., Siegel, D., Rodriguez Jahnke, F., Gerrer, K., Wend, S., Decker, E.L., Reski, R., Weber, W. and Zurbriggen, M.D. (2014) A red light-controlled synthetic gene expression switch for plant systems. *Mol. Biosyst.* **10**, 1679–1688.

Nakamichi, N., Kita, M., Ito, S., Yamashino, T. and Mizuno, T. (2005) PSEUDO-RESPONSE REGULATORS, PRR9, PRR7 and PRR5, together play essential roles close to the circadian clock of *Arabidopsis thaliana*. *Plant Cell Physiol.* **46**, 686–698.

Ordoñez-Herrera, N., Fackendahl, P., Yu, X., Schaefer, S., Koncz, C. and Hoecker, U. (2015) A *cop1 spa* mutant deficient in COP1 and SPA proteins reveals partial co-action of COP1 and SPA during *Arabidopsis* post-embryonic development and photomorphogenesis. *Mol. Plant*, **8**, 479–481.

Osterlund, M.T., Hardtke, C.S., Wei, N. and Deng, X.W. (2000) Targeted destabilization of HY5 during light-regulated development of *Arabidopsis*. *Nature*, **405**, 462–466.

Pacín, M., Legris, M. and Casal, J.J. (2013) COP1 re-accumulates in the nucleus under shade. *Plant J.* **75**, 631–641.

Pacín, M., Legris, M. and Casal, J.J. (2014) Rapid decline in nuclear COSTITUTIVE PHOTOMORPHOGENESIS1 abundance anticipates the stabilization of Its target ELONGATED HYPOCOTYL5 in the light. *Plant Physiol.* **164**, 1134–1138.

Paik, I. and Huq, E. (2019) Plant photoreceptors: multi-functional sensory proteins and their signaling networks. *Semin. Cell Dev. Biol.* **92**, 114–121.

Park, E., Park, J., Kim, J., Nagatani, A., Lagarias, J.C. and Choi, G. (2012) Phytochrome B inhibits binding of PHYTOCHROME INTERACTING FACTORs to their target promoters. *Plant J.* **72**, 537–546.

Park, Y.-J., Lee, H.-J., Ha, J.-H., Kim, J.Y. and Park, C.-M. (2017) COP1 conveys warm temperature information to hypocotyl thermomorphogenesis. *New Phytol.* **215**, 269–280.

Pham, V.N., Xu, X. and Huq, E. (2018) Molecular bases for the constitutive photomorphogenic phenotypes in *Arabidopsis*. *Development*, **145**, dev169870.

Podolec, R. and Ulm, R. (2018) Photoreceptor-mediated regulation of the COP1/SPA E3 ubiquitin ligase. *Curr. Opin. Plant Biol.* **45**, 18–25.

Ponnu, J., Riedel, T., Penner, E., Schrader, A. and Hoecker, U. (2019) Cryptochrome 2 competes with COP1 substrates to repress COP1 ubiquitin ligase activity during *Arabidopsis* photomorphogenesis. *Proc. Natl Acad. Sci. USA*, **116**, 27133–27141.

Reed, J.W., Nagatani, A., Elich, T.D., Fagan, M. and Chory, J. (1994) Phytochrome A and phytochrome B have overlapping but distinct functions in *Arabidopsis* development. *Plant Physiol.* **104**, 1139–1149.

Reed, J.W., Nagpal, P., Poole, D.S., Furuya, M. and Chory, J. (1993) Mutations in the gene for the red/far-red light receptor phytochrome B alter cell elongation and physiological responses throughout *Arabidopsis* development. *Plant Cell*, **5**, 147–157.

Saijo, Y., Zhu, D., Li, J., Rubio, V., Zhou, Z., Shen, Y., Hoecker, U., Wang, H. and Deng, X.W. (2008) Arabidopsis COP1/SPA1 complex and FHY1/FHY3

associate with distinct phosphorylated forms of phytochrome A in balancing light signaling. *Mol. Cell*, **31**, 607–613.

Schneider, C.A., Rasband, W.S. and Eliceiri, K.W. (2012) NIH Image to ImageJ: 25 years of image analysis. *Nat. Methods*, **9**, 671–675.

Seo, H.S., Watanabe, E., Tokutomi, S., Nagatani, A. and Chua, N.-H. (2004) Photoreceptor ubiquitination by COP1 E3 ligase desensitizes phytochrome A signaling. *Genes Dev.* **18**, 617–622.

Seo, H.S., Yang, J.-Y., Ishikawa, M., Bolle, C., Ballesteros, M.L. and Chua, N.-H. (2003) LAF1 ubiquitination by COP1 controls photomorphogenesis and is stimulated by SPA1. *Nature*, **423**, 995–999.

Sheerin, D.J., Menon, C., Oven-Krockhaus, S. *et al.* (2015) Light-activated phytochrome A and B interact with members of the SPA family to promote photomorphogenesis in Arabidopsis by reorganizing the COP1/SPA complex. *Plant Cell*, **27**, 189–201.

Shen, H., Moon, J. and Huq, E. (2005) PIF1 is regulated by light-mediated degradation through the ubiquitin-26S proteasome pathway to optimize photomorphogenesis of seedlings in Arabidopsis. *Plant J.* **44**, 1023–1035.

Shen, H., Zhu, L., Castillon, A., Majee, M., Downie, B. and Huq, E. (2008) Light-induced phosphorylation and degradation of the negative regulator PHYTOCHROME-INTERACTING FACTOR1 from *Arabidopsis* depend upon its direct physical interactions with photoactivated phytochromes. *Plant Cell*, **20**, 1586–1602.

Sievers, F., Wilm, A., Dineen, D. *et al.* (2011) Fast, scalable generation of high-quality protein multiple sequence alignments using Clustal Omega. *Mol. Syst. Biol.* **7**, 539.

Uljon, S., Xu, X., Durzynska, I., Stein, S., Adelmant, G., Marto, J., Pear, W. and Blacklow, S. (2016) Structural basis for substrate selectivity of the E3 Ligase COP1. *Structure*, **24**, 687–696.

Viczián, A., Ádám, É., Wolf, I., Bindics, J., Kircher, S., Heijde, M., Ulm, R., Schäfer, E. and Nagy, F. (2012) A short amino-terminal part of Arabidopsis phytochrome A induces constitutive photomorphogenic response. *Mol. Plant*, **5**, 629–641.

von Arnim, A.G. and Deng, X.-W. (1994) Light inactivation of Arabidopsis photomorphogenic repressor COP1 involves a cell-specific regulation of its nucleocytoplasmic partitioning. *Cell*, **79**, 1035–1045.

Wang, P., Cui, X., Zhao, C. *et al.* (2017) COR27 and COR28 encode nighttime repressors integrating *Arabidopsis* circadian clock and cold response: *COR27* and *COR28* integrate clock and cold signaling. *J. Integr. Plant Biol.* **59**, 78–85.

Waterhouse, A.M., Procter, J.B., Martin, D.M.A., Clamp, M. and Barton, G.J. (2009) Jalview Version 2 – a multiple sequence alignment editor and analysis workbench. *Bioinformatics*, **25**, 1189–1191.

Xu, D. (2019) COP1 and BBXs-HY5-mediated light signal transduction in plants. *New Phytol.* https://doi.org/10.1111/nph.16296.

Yamamoto, Y., Sato, E., Shimizu, T. *et al.* (2003) Comparative genetic studies on the *APRR5* and *APRR7* genes belonging to the APRR1/TOC1 quintet implicated in circadian rhythm, control of flowering time, and early photomorphogenesis. *Plant Cell Physiol.* **44**, 1119–1130.

Yang, H.Q., Tang, R.H. and Cashmore, A.R. (2001) The signaling mechanism of Arabidopsis CRY1 involves direct interaction with COP1. *Plant Cell*, **13**, 2573–2587.

Yu, J.-W.-W., Rubio, V., Lee, N.-Y.-Y. *et al.* (2008) COP1 and ELF3 control circadian function and photoperiodic flowering by regulating GI stability. *Mol. Cell*, **32**, 617–630.

Zhu, L. and Huq, E. (2019) Characterization of light-regulated protein-protein interactions by *in vivo* coimmunoprecipitation (Co-IP) assays in plants. *Methods Mol. Biol.* **2026**, 29–39.